INFRARED SPECTROSCOPY OF THE STRETCHING MODES OF SeH^- AND TeH^- IN KCl AND KBr

C.E. MUNGAN,†‡ U. HAPPEK,†§ T.Z. HOSSAIN,¶ and A.J. SIEVERS†

†Laboratory of Atomic and Solid State Physics and Materials Science Center

¶Ward Laboratory of Nuclear Engineering

Cornell University, Ithaca, NY 14853

Abstract—The fundamental stretching modes near 4.5 μm of SeH^- and TeH^- doped in KCl and KBr are measured at high resolution at 1.7 K. For the KCl-doped samples, prepared by adding elemental Se (Te) to the melt and growing under H_2, the concentrations of atomic Se (Te) are determined by neutron activation analysis. An IR/Raman/UV spectroscopic survey of impurities in these crystals indicates that Se (Te) is present mainly in the form of SeH^- (TeH^-). Thus, ratioing the vibrational absorption strengths to the atomic concentrations gives the integrated cross-sections of SeH^- (TeH^-), equivalent to an effective charge q^* of ~0.14 e and a radiative lifetime of ~30 ms. This value of q^* is much smaller than theoretical predictions for the free ions, implying a matrix-induced screening of the dipole moment. The lowest-order mechanical anharmonic correction to the vibrational frequencies is found to be ~2% by measuring the first overtones and is used to fit the isotopic shifts in the spectral peaks. These peaks are homogeneously broadened at 1.7 K; if lifetime limited, this implies a vibrational relaxation time on the order of 100 ps, nine orders of magnitude faster than the radiative lifetime.

Keywords: A. chalcogenides, B. crystal growth, C. infrared spectroscopy, D. defects, D. optical properties

PACS numbers: 78.50.Ec, 33.70.Ca, 82.80.Jp, 33.70.Fd

---

‡ Present address: Los Alamos National Lab, Mailstop E548, Los Alamos, NM, 87545.
§ Present address: Dept. of Physics and Astronomy, Univ. of Georgia, Athens, Georgia, 30602-2451.

1. INTRODUCTION

The absorption cross-section, σ, and the lowest-order mechanical anharmonic correction, $2x_e\nu_e$, of a vibrational mode of a molecule in a given environment are fundamental quantities directly related to the transition dipole moment and to the nature of the internal chemical bonds of the molecule [1,2]. The values of these two parameters are needed in the analysis of time-resolved optical pumping experiments, since they determine the number of molecules which are pumped up to excited states, the radiative lifetimes of these excited states, whether or not the pump laser is resonant with the overtones of these modes, and the detailed spectral distribution of peaks which arise from the various isotopes of the impurity molecule.

A simple but important class of molecules are the diatomic hydrides, in which hydrogen bonds to another atom. In this respect, the class of molecules in which the other atom is from column VIA of the periodic table (the chalcogens—oxygen through tellurium) are of particular interest because they readily accept an electron and substitutionally replace the anion in ionic hosts such as the alkali halides. Impurity molecules in the alkali halides have been intensively studied since the mid-1960s—see, for example, Barker and Sievers [3]. Recently there has been renewed interest in the diatomic hydrides in particular: Fowler *et al.* have examined the anomalous electrical anharmonicity of OH^- in various insulating solids [4], Otto has measured the electric-field [5] and stress [6] induced splittings of SH^-, SeH^-, and TeH^- in alkali halides, and Heilweil *et al.* [7] and Happek *et al.* [8] have found lifetimes on the order of 100 ps for the vibrational relaxation of OH and SH, respectively, in bulk glasses.

While the vibrational cross-sections and mechanical anharmonicities of OH^- and SH^- in the alkali halides are known [9-11], the corresponding values for SeH^- and TeH^- have not previously been reported in the literature to the best of our knowledge. In this paper, we present high-resolution measurements of the fundamental and overtone spectra of these two molecules doped into KCl and KBr and extract the vibrational mechanical anharmonicities, $2x_e\nu_e$, in the course of which we fit the isotopic shifts in the spectral peak positions. Summing up the absorption strengths of these peaks and dividing by the impurity concentration, as determined by neutron activation analysis, gives the integrated absorption cross-section, σ_{int}. From this, the radiative

lifetimes of the diatomic vibrational modes are computed and compared to the times one obtains by assuming that the homogeneously-broadened absorption peaks have linewidths which are lifetime limited, as is true for SH^- in these same hosts [12]. A nine orders of magnitude difference is found, which suggests the existence of an ultra-rapid nonradiative decay channel for the vibrational relaxation of the diatomic hydrides in the alkali halides.

2. SAMPLE PREPARATION AND CHARACTERIZATION

2.1. *Impurity doping and concentration analysis*

The samples are grown by the Czochralski technique as follows. First, the starting KBr or KCl material is purified by bubbling chlorine gas through it while molten. Next, between 0.04 and 0.4 mol % of powdered elemental selenium or tellurium is added to 100 g of the purified salt. Finally, single crystals are pulled in a partial atmosphere of hydrogen, which reacts with the chalcogen to form SeH^- or TeH^- and is incorporated into the alkali halide matrix [5,13].

Neutron activation analysis is used to determine the total number of selenium or tellurium atoms in a given sample. This analysis is performed in the following manner. A ~30 mm^3 sample of KCl:SeH^- or KCl:TeH^-, whose infrared (IR) spectrum has been previously characterized, is irradiated at a neutron flux of 10^{12} n/s/cm^2 for 3 h at Cornell's TRIGA reactor. After a waiting time of 10 days, which permits the strongly emitting but short-lived ^{38}Cl and most of the ^{42}K isotopes to decay, the rate of gamma ray emission from the long-lived ^{75}Se or ^{131}I (beta-decay product of ^{131}Te) isotopes are measured. From the known neutron flux, capture cross-section, irradiation and waiting times, half-life, and natural isotopic abundances, the atomic concentration of Se or Te in the sample is determined [14]. Note that this technique cannot conveniently be used for KBr doped samples, because the activity of ^{82}Br remains strong even after 10 days.

2.2. *IR/Raman/UV spectroscopic survey of impurities*

The main purpose of this subsection is to demonstrate that the elemental Se (Te) added to the Czochralski melt, as described above, is mainly present in the boules in the form of SeH^- (TeH^-). Other possible species which incorporate chalcogen atoms are discussed below, but no evidence is

found for significant concentrations of them in our samples. Thus, the neutron-activated measurements of the number of selenium (tellurium) atoms in the samples give the SeH^- (TeH^-) concentrations directly, as required for the determination of the cross-sections of these two molecules in Sec. 3.

Infrared spectra of the samples were measured from 400–5000 cm^{-1} at room temperature (RT) and from 800–8000 cm^{-1} at 1.7 K. Other than the fundamental and overtone vibrations of the chalcogen hydrides, to be discussed in detail in Sec. 3, the only other obvious peaks in the spectra were the ν_2 (ν_3) modes of $^{10}BO_2^-$ and $^{11}BO_2^-$ near 600 (2000) cm^{-1} [15]. No evidence for such polyatomic species as H_2Se^-, which has a bending mode near 1000 cm^{-1}, was found [16].

Since O_2^- and S_2^- can substitute for the anions in potassium halide crystals [17,18], it is logical to consider the possibility that Se_2^- and Te_2^- might be present in our samples. Now, $KI{:}Se_2^-$ has a Raman-active vibrational mode at 325 cm^{-1} at RT [19]. Following the suggestions of Schulman and Kirk [18] and of Holzer *et al.* [19], we can estimate the vibrational frequency of Te_2^- at RT as†

$$\frac{\nu(KI{:}Te_2^-)}{\nu(Te_2)} = \frac{\nu(KI{:}Se_2^-)}{\nu(Se_2)} = 0.83, \tag{1}$$

using the gas-phase values of $\nu(Te_2)$ and $\nu(Se_2)$ [16]. This gives $\nu(KI{:}Te_2^-) = 210$ cm^{-1}. We consequently ran Raman spectra of our highest-concentration KCl:Se and KBr:Te samples over the range 40–2600 cm^{-1} at RT in an unpolarized 90° scattering geometry, using the 514.5 nm line of an argon-ion laser. After accounting for host two-phonon sum and difference bands, by comparison with undoped KCl and KBr reference samples, no lines were observed at low frequencies except for a peak at 243 cm^{-1}, together with several of its nearly harmonically spaced overtones, in the case of the KCl:Se sample. We attribute this sequence of lines to the vibrations of Cl_2^- [20,21]. In any case, no peaks corresponding to Se_2^- or Te_2^- were found, for laser power levels of up to 1 W. Note, in particular, that if any Se_2^- molecules were present, we would benefit from a resonant enhancement in the signal, due to the electronic absorption of the molecules at the 514.5 nm laser wavelength, as discussed below.

---

† Note that $\nu(KI{:}S_2^-) / \nu(S_2) = 0.83$, in excellent agreement with Eq. (1).

At larger Stokes-shifted Raman frequencies, the fundamental chalcogen hydride stretching mode can be resolved at RT, provided that the impurity concentration is sufficiently high. For example, the inset plot in Fig. 1 shows the vibrational peak of KCl:SeH$^-$. The center of the line is Lorentzian with a peak frequency ν_{01} of 2321 cm^{-1} and a deconvolved FWHM of 21 cm^{-1}, in excellent agreement with the 19 cm^{-1} wide Lorentzian at 2321 cm^{-1} observed in IR absorption at RT. The wings of the spectra in both cases show additional intensity, especially on the high-frequency side of the lines, which are probably phonon sum and difference bands.

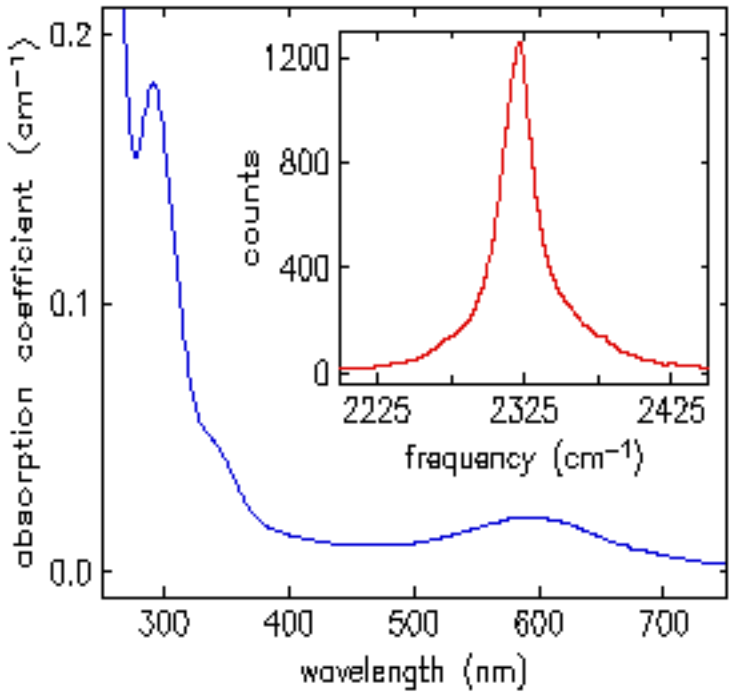

Fig. 1. *Main plot*—Visible and near UV absorption spectrum of a KCl+Te+H_2 boule at RT and 5 nm resolution. The off-scale absorption at the shortest wavelengths is the far wing of the very strong electronic absorption peaks at ~200 nm of the chalcogen hydride molecules. *Inset*—Background-corrected Stokes Raman spectrum of the fundamental vibrational mode of KCl:SeH$^-$ at RT and 17 cm^{-1} resolution.

Upper limits on the amounts of Se_2^- and Te_2^- in the samples can be found by looking for their lowest-energy electronic excitations, in the visible (VIS) region of the electromagnetic spectrum. It is known that O_2^- has a broad absorption band at 250 nm [22], S_2^- at 400 nm [18], Se_2^- near 500 nm [23], and hence, by extension of this trend, Te_2^- might be expected to absorb around 600 nm. Room temperature UV/VIS/NIR spectra were run from 3000 nm (i.e., 3300 cm^{-1}, which overlaps with the IR spectra mentioned above) down to 180 nm. The main plot in Fig. 1 shows a portion of this spectrum for the entire lower half of the KCl:Te:H_2 boule. This

long sample has a blue tint, caused by the the 140 nm wide line which peaks at 590 nm in the figure. Although we cannot firmly rule out the possibility that part of this absorption might be due to *F* centers, whose peak lies at 565 nm in KCl at RT [24], this is unlikely for several reasons. First of all, an almost identical band, displaced by no more than 5 nm, is found for KBr:Te:H_2, in striking contrast to the 70 nm Mollwo-Ivey shift of the *F* center peak in KBr compared to KCl [24]. Secondly, the reaction of Se and H_2 to form SeH^- during the crystal growth requires electrons, making it unlikely that free electrons would be available to create *F* centers. Finally, Cl_2^- centers are strong electron traps and readily annihilate with any available *F* centers [24].

Thus, we cannot rule out the possibility that the 590 nm in Fig. 1 is due to KCl:Te_2^- centers. In such a case, by integrating the strength of the line and applying the Smakula equation [24], we can determine the concentration of these centers in a sample. In the absence of any specific knowledge of the oscillator strength of the UV absorption of KCl:Te_2^-, we use the value 0.17, which we calculate for the 243 nm absorption band of KCl:O_2^- from Fischer *et al.*'s [25] calibrated spectral measurements.† Doubling the resulting concentration of Te_2^-, to find the number of Te atoms involved, and ratioing to the *total* concentration of Te in the sample, as measured by neutron activation analysis, indicates that no more than 4.5% of the tellurium is in the form of Te_2^- rather than TeH^-. This is, at worst, a small error in our determination of the cross-section of TeH^- in Sec. 3.2 below.

In the case of the KCl:Se:H_2 boule, a weak 95 nm wide line is found at 515 nm, giving rise to an overall light pink color. At least some of this band definitely arises from Cl_2^- centers [26] and hence we can only establish an upper limit on the amount of Se_2^- present, by integrating the absorption intensity of this line. Taking the oscillator strength to again be 0.17, we find that no more than 0.06% of the Se atoms occur in this diatomic form, a completely negligible amount.

The absence of significant concentrations of Se_2^- and Te_2^- centers in our KCl and KBr samples is perhaps not surprising, in light of the large size [27] of these diatomics relative to that of Cl^- and Br^-. In fact, Holzer *et al.* [19] comment that they were unable to diffuse a significant

---

† The relevant parameters corresponding to Fig. 2 of Ref. [25] are: peak absorption coefficient of 45 cm^{-1}, FWHM of 1.2 eV, and O_2^- concentration of 3.1 x 10^{18} cm^{-3}.

concentration of S_2^- into KCl for this very reason, nor were Vannotti and Morton [28] able to introduce Se_2^- into KCl or KBr. Furthermore, these latter authors suggest that Se_2^- centers may actually thermally decompose under long-term exposure to visible light.

Another possible chemical form which the elemental chalcogen could adopt in the crystals is that of colloids [29]. The resulting small particles, if approximated as a dilute concentration of small (compared to visible wavelengths) spheres with filling fraction *f*, give rise from Mie theory to a sphere resonance. The absorption coefficient, α, describing this resonance is [29]

$$\alpha = 18\pi f \nu (\varepsilon_\infty^{\text{host}})^{3/2} \frac{\varepsilon_2}{(\varepsilon_1 + 2\varepsilon_\infty^{\text{host}})^{3/2} + \varepsilon_2^2}, \tag{2}$$

where ν is the frequency of light in cm^{-1}, $\varepsilon_\infty^{\text{host}}$ equals 2.19 for KCl [30], and $\varepsilon_1 = n^2 - k^2$ and $\varepsilon_2 = 2nk$, with *n* and *k* the real and imaginary parts of the refractive index of Se or Te, as appropriate. The crystalline forms of these two elements are birefringent and it is necessary to distinguish *n* and *k* in the parallel (extraordinary) and perpendicular (ordinary) directions to the *c* axis, as tabulated by Palik [31].

For tellurium in KCl, we find that the sphere resonance peaks at 295 nm with a width of 50 nm for light propagating along the *c* axis, and at 325 nm with FWHM = 80 nm in the perpendicular plane. These *may* correspond to the 30 nm wide line at 295 nm and the 50 nm wide weaker band at 345 nm in Fig. 1. Assuming that this is the case, we compute the overall colloidal absorption profile as $(\alpha_\parallel + 2\alpha\ )/\ 3$ and choose *f* in Eq. (2) to make its integrated intensity match the area under the two peaks in Fig. 1 (after correcting for the sloping background in this spectral region). Using the known density and mass of crystalline Te to convert this filling fraction to an atomic concentration, we find that no more than 6.4% of the Te atoms in this sample are present in colloidal form.

In the case of KCl:Se, the sphere resonances in the parallel and perpendicular directions have very similar peak positions and widths, namely about 255 nm and 55 nm, respectively. A 26 nm wide line is found at 231 nm, in the long wavelength wing of the SeH^- 197 nm absorption band discussed below. This 231 nm line has been seen by Fischer [13], who attributed it to an unspecified internal transition of the SeH^- molecule since an analogous peak also occurs for SH^-

[32]. Therefore, the area of this band is likely to be an overestimate for the strength of the sphere resonance, but implies that, at absolute most, 7.3% of the Se atoms are in colloidal form.

Finally, to complete our spectroscopic survey of the samples, we discuss the ~200 nm electronic absorption peaks of the chalcogen hydrides. Fischer has previously measured these optical transitions for SeH^- and TeH^- in various alkali halides as a function of temperature [13] and found a doublet, arising from spin-orbit splitting, at low temperatures, which merges at RT into a single asymmetric line, peaking at 197 nm for KCl:SeH^- and at somewhat longer wavelengths for TeH^-. We were able to reproduce his RT spectrum for KCl:SeH^- in the 5–6.5 eV range by polishing a sliver of one of the neutron-activation samples down to a thickness of 250 μm. From this, we determine the UV oscillator strength to be 0.30, not including the (small) intensity of the poorly-understood 231 nm shoulder peak mentioned in the preceding paragraph. This can be compared to 0.13 for the UV oscillator strength of KCl:OH^- [33] which peaks at RT at 204 nm [34], and to 0.21 which we calculate from Fischer and Gründig's data for KCl:SH^- [32] with a RT absorption maximum at 188 nm [35]. Note that OH^- and SH^- do not show a doublet at low temperatures because their spin-orbit coupling constants are small [13]. We estimate that the UV oscillator strength of KCl:TeH^- is ~0.30 and that it peaks at ~210 nm at RT, where the uncertainties here arise from the contaminating presence of roughly 25 ppm of SH^-, as observed in the low-temperature IR spectra of this particular sample.

3. IR SPECTROSCOPY OF THE VIBRATIONAL MODES

3.1. *Stretching modes of* SeH^-

The blue curve in Fig. 2 shows the measured IR absorption spectrum in the region of the fundamental stretching mode of KBr:SeH^- near 2300 cm^{-1} (4.3 μm) at 1.7 K with 0.04 cm^{-1} resolution. The linewidth (FWHM) of the strongest peak at 2305.43 cm^{-1}, corresponding to the most abundant $^{80}SeH^-$ isotope (cf. Table 1), is only† $\gamma = 0.085$ cm^{-1}. Since its lineshape is well described by a Lorentzian, the broadening is mostly homogeneous, and hence the total vibrational dephasing time is given by $T_2 = 1/\pi c\gamma = 125$ ps. If the pure dephasing time, T_2^*, is much longer

† The instrumental resolution has been deconvolved in quadrature from the measured linewidth.

than the vibrational relaxation time, T_1, as we showed to be true [36] for the fundamental vibration of SH^- in KI at 1.7 K by comparing the value of T_2 measured by persistent spectral hole burning to that of T_1 measured by incoherent saturation, then $T_1 \quad T_2 / 2$. This suggests that the vibrational relaxation time of SeH^- in the alkali halides at low temperatures is on the order of 100 ps, comparable to what we have previously measured for SH^- in these same hosts [12].

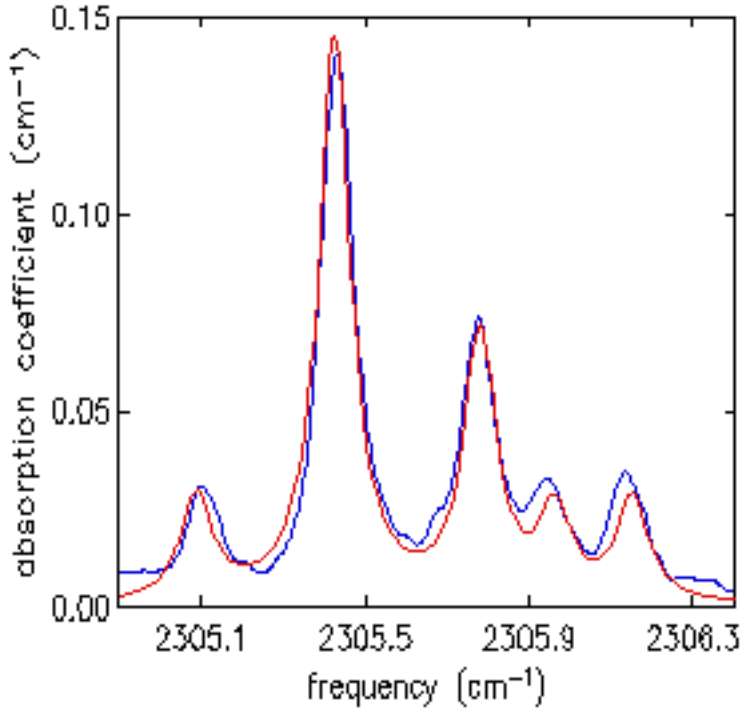

Fig. 2. Absorption spectrum (blue curve) of the fundamental vibrational modes of KBr:SeH^- at 1.7 K and 0.04 cm^{-1} resolution. The red curve is the sum of six Lorentzians, whose peak frequencies are determined from Eq. (4) and are listed in Table 1, whose undeconvolved widths (FWHM) are 0.095 cm^{-1}, and whose heights are (0.145 cm^{-1}) x (^{i}A / ^{80}A), where ^{i}A is the natural abundance of isotope ^{i}Se from Table 1.

When SeH^- is doped into KCl, the strong $^{80}SeH^-$ peak is found at ν_{01} = 2322.9 cm^{-1} at 1.7 K, almost identical to the positions of the IR and Raman maxima at RT mentioned in Sec. 2.2, but slightly higher in frequency than that of KBr:$^{80}SeH^-$ (cf. Fig. 2). This frequency is near the peak of the roto-vibrational spectrum of atmospheric CO_2, which tends to interfere with the measurements even after pumping out the interferometer to a pressure of 1 torr. However, the first vibrational overtone, $0 \rightarrow 2$, of KCl:SeH^- can be cleanly resolved at 1.7 K (blue curve in Fig. 3). The dominant $^{80}SeH^-$ peak is at ν_{02} = 4558.9 cm^{-1}. The lowest-order mechanical anharmonic correction to the vibrational term values is [1]

$$2x_e\nu_e = 2\nu_{01} - \nu_{02}, \tag{3}$$

which is equal to 87 cm^{-1}. Note that this value implies that $\nu_e = \nu_{01} + 2x_e\nu_e$ equals 2410 cm^{-1} for KCl:SeH$^-$ and 2392 cm^{-1} for KBr:SeH$^-$, in excellent agreement with ν_e = 2400 ± 50 cm^{-1} observed for the free SeH radical in its electronic ground state [37].

Table 1. Peak frequencies of the fundamental stretching modes of the isotopes of KBr:SeH$^-$ at 1.7 K. The measured values are from the blue curve in Fig. 2 and the calculated values are obtained using Eq. (4), giving the red curve in Fig. 2, where the peak heights have been scaled according to the natural isotopic abundances of Se listed in the second column.

Isotopic Impurity	Natural Abundance (%)	Measured Frequency (cm^{-1})	Calculated Frequency (cm^{-1})
^{82}SeH$^-$	9.2	2305.10	2305.09
^{80}SeH$^-$	49.8	2305.43	2305.43
^{78}SeH$^-$	23.5	2305.78	2305.78
^{77}SeH$^-$	7.6	2305.95	2305.96
^{76}SeH$^-$	9.0	2306.14	2306.15
^{74}SeH$^-$	0.9	–	2306.55

Knowing the fundamental frequency of the dominant isotope, ν_{01}, and the mechanical anharmonicity, $2x_e\nu_e$, we can calculate the fundamental and overtone frequencies of any other isotope *i*, ν_{01}^i and ν_{02}^i, respectively, as [1]

$$\begin{aligned} \nu_{01}^i &= \rho\nu_{01} + (\rho - \rho^2)2x_e\nu_e \\ \nu_{02}^i &= 2\rho\nu_{01} + (2\rho - 3\rho^2)2x_e\nu_e \end{aligned} \tag{4}$$

where $\rho = (\mu / \mu^i)^{1/2}$, with μ and μ^i the reduced masses of ^{80}SeH$^-$ and of ^{i}SeH$^-$, respectively. The red curves in Figs. 2–3 were obtained by positioning a Lorentzian at each of these frequencies. For example, the calculated frequencies for KBr:SeH$^-$, corresponding to Fig. 2, are listed in Table 1. There are two free parameters in each fit in the figures: the width and height of the dominant peak. The other peaks have the same width, and heights which scale linearly with the natural abundances of the isotopes. In comparison to the fundamental vibrational lines of SeH$^-$ in Fig. 2,

notice that the overtone peaks in Fig. 3 are spaced twice as far apart, as expected from Eq. (4). In addition, the overtone lines are roughly twice as broad as the fundamental ones. If these lines are lifetime broadened, as we argued for the fundamental peaks, then molecules in the second excited state must be relaxing twice as fast as those in the first excited state. This is to be expected if the coupling between the impurity vibration and its energy accepting modes is linear, just as we have recently discovered for the vibrational relaxation of CN^- into local modes [38].

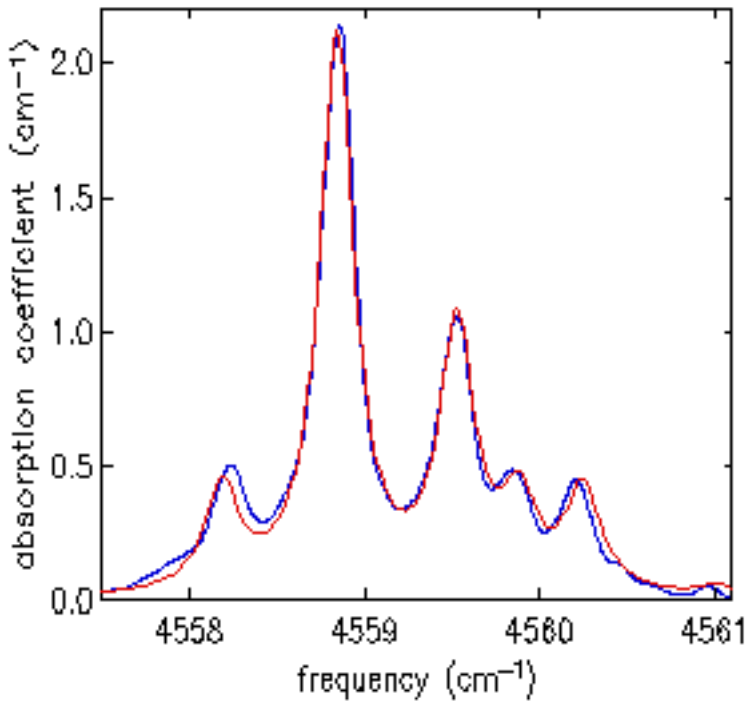

Fig. 3. Absorption spectrum (blue curve) of the first overtone of the vibrational modes of KCl:SeH^- at 1.7 K and 0.1 cm^{-1} resolution. The red curve is the sum of six Lorentzians, whose peak frequencies are obtained from Eq. (4), whose undeconvolved widths (FWHM) are 0.24 cm^{-1}, and whose heights are (2.1 cm^{-1}) x (^{i}A / ^{80}A), where ^{i}A is the natural abundance of isotope ^{i}Se, as listed in Table 1.

Two small samples of KCl:SeH^- were cleaved from the same part of the boule. Their fundamental absorption strengths, integrated over all isotopes, were S_{01} = 17 ± 1 cm^{-2} (measured at room temperature, since the peaks are immeasurably strong at low temperatures). The average selenium concentration in the two pieces was found by neutron activation analysis to be 0.0233 ± 0.0015 mol %, which corresponds to a SeH^- concentration, N, of 3.75 x 10^{18} cm^{-3}, assuming that no Se is present in colloidal form. The integrated absorption cross-section is defined as [11,39]

$$\sigma_{int} = \frac{S_{01}}{N} = \frac{(q^*)^2 \pi}{3\mu c^2} \frac{(n^2+2)^2}{9n}, \tag{5}$$

where q^* is the effective charge† and n is the refractive index of the host. The dependence on n arises from the Lorentz local-field correction and reflects the enhanced absorption of a molecule in a dielectric medium, relative to that of one in free space. Equation (5) implies σ_{int}(KCl:SeH$^-$) = (4.5 ± 0.6) x 10^{-18} cm, or equivalently, q^* = 0.145 ± 0.010 e. This can be compared to q^*(KCl:OH$^-$) = 0.12 ± 0.02 e [9] and q^*(KCl:SH$^-$) = 0.09 ± 0.01 e [11]. The radiative lifetime of the fundamental stretching mode is related to this integrated cross-section according to [39]

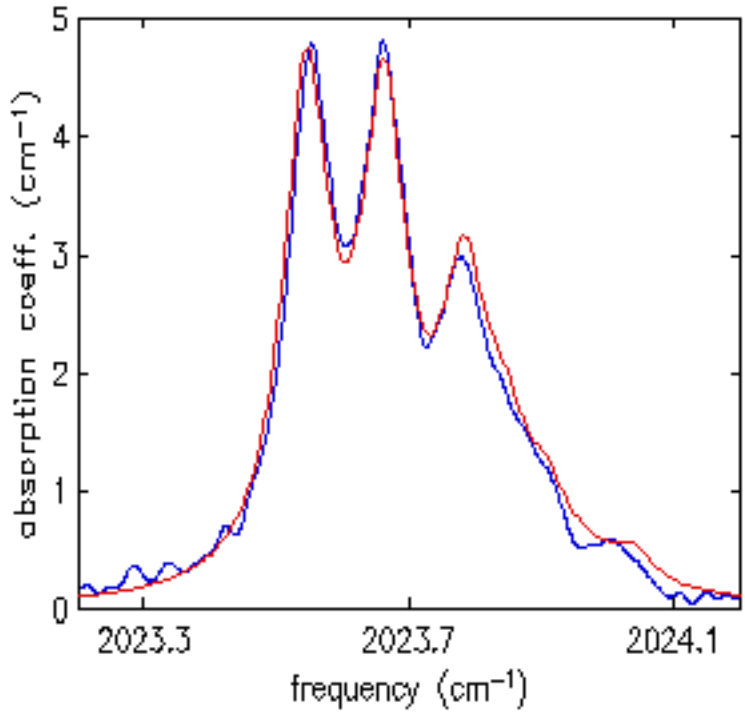

Fig. 4. Absorption spectrum (blue curve) of the fundamental vibrational modes of KBr:TeH$^-$ at 1.7 K and 0.02 cm^{-1} resolution. The red curve is the sum of eight Lorentzians, whose peak frequencies are calculated using Eq. (4) and are listed in Table 2, whose undeconvolved widths (FWHM) are 0.085 cm^{-1}, and whose heights are (4.2 cm^{-1}) x (^iA / ^{130}A), where ^iA is the natural abundance of isotope ^{i}Te in Table 2.

$$\tau_{rad} = \left[8\pi n^2 c \nu_{01}^2 \sigma_{int}\right]^{-1} \tag{6}$$

from which we find τ_{rad}(KCl:SeH$^-$) = 25 ms.

3.2. *Stretching modes of* TeH$^-$

Figure 4 shows the fundamental IR absorption spectrum of TeH$^-$ doped in KBr at 1.7 K with 0.02 cm^{-1} resolution. The lowest-frequency peak at ν_{01} = 2023.55 cm^{-1} is that of the most abundant isotope, namely ^{130}TeH$^-$ (cf. Table 2). The overtone is at ν_{02} = 3972.9 cm^{-1}, and hence $2x_e\nu_e$ = 74 cm^{-1} from Eq. (3). This can be compared to $2x_e\nu_e$ = 80 cm^{-1} and $\nu_{01} = \nu_e - 2x_e\nu_e$ = 2057

† The oscillator strength is equal to $(q^*/e)^2/3$.

cm^{-1} for the free ^{130}TeH radical [40]. As before, we use these values of the mechanical anharmonicity and of the dominant isotopic frequency to calculate the fundamental vibrational frequencies of all the other isotopes, using Eq. (4). The results are listed in Table 2. The sum of a set of Lorentzians is found to best fit the experimental spectrum, giving the red curve in Fig. 4, where the peak heights are scaled according to the natural abundances and each peak is chosen to have a FWHM of 0.085 cm^{-1}. If this homogeneous width is lifetime-limited, as we argued above for KBr:SeH$^-$, then we again find that T_1 must be on the order of 100 ps.

Table 2. Peak frequencies of the fundamental stretching modes of the isotopes of KBr:TeH$^-$ at 1.7 K. The measured values are from the blue curve in Fig. 4 (the two values marked with a tilde are barely perceivable as weak bumps on the right-hand side of the curve) and the calculated values are obtained using Eq. (4), giving the red curve in Fig. 4, where the peak heights have been scaled according to the natural isotopic abundances of Te listed in the second column.

Isotopic Impurity	Natural Abundance (%)	Measured Frequency (cm^{-1})	Calculated Frequency (cm^{-1})
^{130}TeH$^-$	34.5	2023.55	2023.55
^{128}TeH$^-$	31.7	2023.66	2023.66
^{126}TeH$^-$	18.7	2023.78	2023.78
^{125}TeH$^-$	7.0	~2023.84	2023.85
^{124}TeH$^-$	4.6	~2023.91	2023.91
^{123}TeH$^-$	0.9	–	2023.97
^{122}TeH$^-$	2.5	2024.00	2024.04
^{120}TeH$^-$	0.1	–	2024.17

In KCl, the TeH$^-$ fundamental stretching mode is at ν_{01} = 2043.4 cm^{-1} at 1.7 K, and it overlaps with the $^{10}BO_2^-$ ν_3 = 2046.6 cm^{-1} vibrational mode [15] at higher temperatures. It only proves possible to grow a crystal with a small TeH$^-$ concentration, because of the much larger ionic radius of tellurium than of chlorine [27], and hence the overtone is barely detectable at

ν_{02} = 4014.0 cm^{-1}. These values of ν_{01} and ν_{02} imply $2x_e\nu_e$ = 73 cm^{-1}, in good agreement with what was found for KBr:TeH$^-$ above. The fundamental absorption strength,† integrated over all isotopes, is 0.095 ± 0.005 cm^{-2} and the average concentration, as determined by neutron activation analysis, for two samples from the same part of the boule is (1.55 ± 0.10) x 10^{-4} mol %. Using Eq. (5), these values give σ_{int}(KCl:TeH$^-$) = (3.8 ± 0.5) x 10^{-18} cm, or alternatively, q^* = 0.135 ± 0.010 e, again neglecting any possible colloidal or diatomic tellurium. This in turn implies that τ_{rad}(KCl:TeH$^-$) = 40 ms from Eq. (6), comparable to what we found for KCl:SeH$^-$ above.

4. DISCUSSION OF CHALCOGEN HYDRIDE VIBRATIONAL PARAMETERS

In Table 3, we have summarized the values of the mechanical anharmonicities and effective charges measured for four different diatomic hydrides in KCl, together with some other relevant parameters. It can be seen that the vibrational frequency, ν_{01}, systematically decreases as the chalcogen atomic number increases. This implies that the internal chemical bond of the impurity molecules grows progressively weaker, which correlates well with the decreasing ionic character of the bond as measured by the difference in electronegativity of the chalcogen atom and the hydrogen atom (which has a Pauling electronegativity [27] of 2.1).

The vibrational mechanical anharmonicity can be expressed in fractional form as x_e, which can be calculated from $2x_e\nu_e$, using the fact [1] that $\nu_e = \nu_{01} + 2x_e\nu_e$. For the homologous chalcogen hydrides, the bonds are found to have comparable mechanical anharmonicities, namely about 2%, decreasing only slightly as one descends Table 3.

In contrast to this monotonic decrease in the vibrational frequencies and in the mechanical anharmonicities with increasing chalcogen atomic weight, no simple trend is apparent for the experimental values of the effective charge, q^*, in Table 3. This might be explained as follows. Cade's theoretical calculations [41] of the dipole moment functions (d.m.f.) for *free* OH$^-$ and SH$^-$ can be used to calculate q^*, assuming that the molecular center of mass (c.o.m.) resides at the lattice site. (See, for example, Wedding and Klein [9] for an explanation of this calculation for the

† We explicitly verified for this sample that the absorption strength at 1.7 K is equal to that at 300 K, by carefully fitting and subtracting out the relatively sharp $^{10}BO_2^-$ peak in the RT spectrum.

case of OH^-, noting that q^* is just equal to the absolute value of the derivative of the on-center d.m.f.) We assume that the d.m.f. of SeH^- and TeH^- are roughly equal to that of SH^-, since these three molecules have similar electronegativities and <111> equilibrium orientations, in contrast to the significantly larger electronegativity of OH^- (cf. Table 3) and its <100> orientation. Using this assumption, together with the equilibrium bondlengths [42] listed in Table 3 (which agree, for OH^- and SH^-, with Cade's theoretical results to better than 0.02 Å), we find that q^* ought to increase monotonically with increasing chalcogen atomic number. The reason for this is that the decrease in the derivative of the d.m.f. (evaluated at the geometric center of the molecule) with increasing bondlength is more than compensated for by the shift of the geometric center of the charged molecule away from the c.o.m. (and hence from the lattice site) with increasing chalcogen atomic weight.

Table 3. Various parameters which characterize four homologous impurity molecules doped into KCl at low concentrations. The second column gives the peak frequency of the most abundant isotope at 1.7 K; the third gives the Pauling electronegativity [27] of the chalcogen atom X = O, S, Se, or Te; the fourth column lists the vibrational mechanical anharmonicity; the fifth gives the experimental values of the effective charge, as determined from the absorption strengths and impurity concentrations using Eq. (5); the sixth lists the molecular bondlength, estimated as the X-H bondlength of free H_2X [42]; and finally, the seventh and eighth columns give theoretical values of the effective charge, determined from calculations of the dipole moment functions of free OH^- and SH^- in the indicated references.

Molecule	ν_{01} (cm^{-1})	Chalcogen e.n.	$2x_e\nu_e$ (cm^{-1})	Experimental q^* (e)	Bond-length (Å)	Calculated q^* (e) Ref.[41]	Refs.[43,44]
OH^-	3642.1	3.5	171 [9]	0.12 [9]	0.96	0.14	0.27
SH^-	2591.3	2.5	99 [10]	0.09 [11]	1.34	0.21	0.30
SeH^-	2322.9	2.4	87	0.145	1.46	0.30	0.38
TeH^-	2043.4	2.1	73	0.135	1.66	0.43	0.47

More recent and accurate calculations of the d.m.f. of free OH^- [43] and SH^- [44] by Werner *et al*. give notably larger values of q^* (cf. last two columns of Table 3). The difference arises from the fact that in the newer calculations the molecular d.m.f. peaks at much shorter values of the bondlength than Cade's results suggested.

The resulting theoretical values of q^* are much larger than the corresponding experimental values (cf. Table 3). Otto [11] argues that this reduction in the values of q^* for the alkali-halide-doped molecules compared to the free species is due to a matrix-induced change in the internal charge distribution of the molecules. This is supported by his finding that q^* for SH^- increases as the host lattice constant increases and hence the interactions between the impurity and the surrounding host grow weaker. Wedding and Klein [9] earlier proposed a similar idea to explain the anomalously small oscillator strengths of OH^- and OD^- in the sodium halides. They suggested that the four nonbonding electrons in the outer shell of the chalcogen ion shift (upon matrix substitution) by an amount which depends upon the host crystal lattice. In particular, we notice that their data indicates that q^* increases monotonically in the order NaCl:OH^-, KCl:OH^-, and RbCl:OH^-. In fact, this trend continues for the spacious CsCl:OH^- lattice, using Krantz and Lüty's measurement of the vibrational oscillator strength of this system [45].

The larger experimental value of q^* for OH^- than SH^- is opposite to the theoretical trend in Table 3 for either Cade's or Werner's results. This could arise from an off-center position of OH^- in KCl, an idea which has been extensively but inconclusively discussed in the literature. For example, Bron and Dreyfus [46] estimate that the c.o.m. of the molecule is displaced from the lattice site by 0.34 Å. In that case, the geometric center of the molecule would be almost coincident with the lattice site, and the theoretical values for q^* for OH^- would then be larger than those for SH^-.

Finally, the slightly smaller experimental value of q^* for TeH^- compared to SeH^- in Table 3 might be a result of the tight fit of the large TeH^- molecule in KCl. The Cl^- ion has a crystal radius of only 1.81 Å, in contrast to the 2.21 Å size of Te^{2-} [27]. This would tend to result in outward displacements of the ion cores and electron shells of the surrounding K^+ nearest neighbors, with a consequent change in the induced dipole moment of the TeH^- molecule. In support of this idea,

recent calculations by Hermansson [47] indicate that internal electric fields can significantly alter the derivative of the dipole moment of a diatomic hydride in an ionic lattice. This, again, may have an important bearing on the question of why the experimental oscillator strengths of the matrix-substituted hydrides are so much smaller than the theoretical values for the free ions.

5. SUMMARY

The key results presented in this paper are as follows:

1. Single crystals of SeH^- (TeH^-) in KCl or KBr, prepared by adding elemental Se (Te) to the salt and growing under H_2, are found to be almost completely free of other possible Se (Te) containing species. In particular, molecules such as H_2Se^- (H_2Te^-) and Se_2^- are not present (although a small concentration of Te_2^- cannot be ruled out), and, at most, 7% of the Se (Te) atoms in the boules are in colloidal form. The strongest peaks observed in the UV/VIS spectra at RT are those due to electronic absorptions of SeH^- and TeH^- at roughly 197 and 210 nm for KCl, respectively, with an oscillator strength of ~0.30.
2. From the calibrated IR absorption spectra, the fractional charge participating in the fundamental stretching vibrations of SeH^- and TeH^- doped in KCl is found to be $q^* \approx 0.14\ e$. Theoretical calculations predict much larger values, neglecting any possible matrix-induced screening of the effective charge transferred across the internal molecular bond.
3. These experimental values of q^* lead to a radiative lifetime for vibrational relaxation from levels $1 \rightarrow 0$ of ~30 ms. However, if the homogeneously broadened absorption lines have a lifetime-limited width, then $T_1 \approx 100$ ps. This suggests the existence of an unidentified ultrafast nonradiative mechanism for the vibrational relaxation of the matrix-isolated diatomic hydrides.
4. The molecular bonds for four different KCl-doped chalcogen hydrides are found to have ~2% mechanical anharmonic character from measurements of the the first vibrational overtone spectra. It is necessary to know these anharmonicities in order to fully predict the isotopic shifts in the peak stretching frequencies.

Acknowledgements—This work is supported by NSF-DMR-9312381, ARO-DAAL03-92-G-0369, and NASA-NAGW-2768. In addition, this research made use of the MRL Facilities supported by the National Science Foundation under Award No. DMR-9121654.

REFERENCES

1. Herzberg G., *Molecular Spectra and Molecular Structure I. Spectra of Diatomic Molecules*, 2nd ed. Van Nostrand, NY (1953), Chap. III.
2. Loudon R., *The Quantum Theory of Light*, 2nd ed. Clarendon Press, Oxford (1990).
3. Barker A.S. Jr. and Sievers A.J., *Rev. Mod. Phys.* **47**, Suppl. 2, S1 (1975).
4. Fowler W.B., Capelletti R., and Colombi E., *Phys. Rev. B* **44**, 2961 (1991); Woll A.R. and Fowler W.B., *Phys. Rev. B* **48**, 16788 (1993).
5. Otto J., *Phys. Stat. Sol. (b)* **151**, 363 (1989).
6. Otto J., *Phys. Stat. Sol. (b)* **148**, 489 (1988).
7. Heilweil E.J., Casassa M.P., Cavanagh R.R., and Stephenson J.C., *Chem. Phys. Lett.* **117**, 185 (1985).
8. Happek U., Engholm J.R., and Sievers A.J., *Chem. Phys. Lett.* **221**, 279 (1994).
9. Wedding B. and Klein M.V., *Phys. Rev.* **177**, 1274 (1969).
10. Chi C.-K. and Nixon E.R., *J. Phys. Chem. Solids* **33**, 2101 (1972).
11. Otto J., *Phys. Stat. Sol. (b)* **142**, 105 (1987).
12. Mungan C.E., Happek U., McWhirter J.T., and Sievers A.J., in *Defects in Insulating Materials* (Edited by O. Kanert and J.-M. Spaeth), p. 536. World Scientific, Singapore (1993), Vol. 1.
13. Fischer F., *Z. Physik* **187**, 262 (1965); Fischer F., *Naturwissenschaften* **54**, 313 (1967).
14. Erdtmann G. and Petri H., in *Treatise on Analytical Chemistry* (Edited by P.J. Elving, V. Krivan, and I.M. Kolthoff), Part I, Vol. 14, 2nd ed., p. 520. John Wiley, NY (1986).
15. Hisatsune I.C. and Suarez N.H., *Inorg. Chem.* **3**, 168 (1964).
16. Nakamoto K., *Infrared and Raman Spectra of Inorganic and Coordination Compounds*, 4th ed. Wiley, NY (1986), Chap. II.
17. Känzig W. and Cohen M.H., *Phys. Rev. Lett.* **3**, 509 (1959).
18. Schulman J.H. and Kirk R.D., *Solid State Commun.* **2**, 105 (1964).
19. Holzer W., Murphy W.F., and Bernstein H.J., *J. Mol. Spectrosc.* **32**, 13 (1969).

20. Howard W.F. Jr. and Andrews L., *J. Am. Chem. Soc.* **95**, 2056 (1973).

21. Goovaerts E. and Schoemaker D., *Phys. Stat. Sol. (b)* **88**, 615 (1978).

22. Rolfe J., Lipsett F.R., and King W.J., *Phys. Rev.* **123**, 447 (1961).

23. Vella G.J. and Rolfe J., *J. Chem. Phys.* **61**, 41 (1974).

24. Schulman J.H. and Compton W.D., *Color Centers in Solids*. Pergamon Press, NY (1962), Chaps. III-IV.

25. Fischer F., Gründig H., and Hilsch R., *Z. Physik* **189**, 79 (1966).

26. Delbecq C.J., Kolopus J.L., Yasaitis E.L., and Yuster P.H., *Phys. Rev.* **154**, 866 (1967).

27. Pauling L., *General Chemistry*. Dover, NY (1988), Chap. 6.

28. Vannotti L.E. and Morton J.R., *J. Chem. Phys.* **47**, 4210 (1967).

29. Hughes A.E. and Jain S.C., *Ann. Physik* **28**, 717 (1979).

30. Knox R.S. and Teegarden K.J., in *Physics of Color Centers* (Edited by W.B. Fowler), p. 625. Academic Press, NY (1968).

31. Palik E.D., in *Handbook of Optical Constants of Solids II* (Edited by E.D. Palik), p. 691. Academic Press, San Diego (1991); Palik E.D., *ibid.*, p. 709.

32. Fischer F. and Gründig H., *Z. Physik* **184**, 299 (1965).

33. Fritz B., Lüty F., and Anger J., *Z. Physik* **174**, 240 (1963).

34. Etzel H.W. and Patterson D.A., *Phys. Rev.* **112**, 1112 (1958).

35. Rolfe J., *Appl. Phys. Lett.* **6**, 66 (1965).

36. Mungan C.E. and Sievers A.J., *J. Opt. Soc. Am. B* **9**, 746 (1992).

37. Lindgren B., *J. Mol. Spectrosc.* **28**, 536 (1968).

38. Happek U., Mungan C.E., von der Osten W., and Sievers A.J., *Phys. Rev. Lett.* **72**, 3903 (1994).

39. Di Bartolo B., *Optical Interactions in Solids*, p. 410. John Wiley, NY (1968).

40. Fink E.H., Setzer K.D., Ramsay D.A., and Vervloet M., *J. Mol. Spectrosc.* **138**, 19 (1989).

41. Cade P.E., *J. Chem. Phys.* **47**, 2390 (1967).

42. Callomon J.H., Hirota E., Kuchitsu K., Lafferty W.J., Maki A.G., and Pote C.S., *Structure Data of Free Polyatomic Molecules* (Edited by K.-H. Hellwege and A.M. Hellwege), Landolt-

Börnstein, Vol. II/7. Springer-Verlag, Berlin (1976), Chap. 2.

43. Werner H.-J., Rosmus P., and Reinsch E.-A., *J. Chem. Phys.* **79**, 905 (1983).
44. Senekowitsch J., Werner H.-J., Rosmus P., Reinsch E.-A., and ONeill S.V., *J. Chem. Phys.* **83**, 4661 (1985).
45. Krantz M. and Lüty F., *Phys. Rev. B* **37**, 7038 (1988).
46. Bron W.E. and Dreyfus R.W., *Phys. Rev.* **163**, 304 (1967).
47. Hermansson K., *Int. J. Quantum Chem.* **45**, 747 (1993).